Available online at www.sciencedirect.com
ScienceDirect
Catalysis Today 123 (2007) 189–197
CATALYSIS TODAY
www.elsevier.com/locate/cattod

Kinetics of propylene epoxidation using H_2 and O_2 over a gold/mesoporous titanosilicate catalyst

Jiqing Lu [a,b], Xiaoming Zhang [a,c], Juan J. Bravo-Suárez [a], Susumu Tsubota [a], Jason Gaudet [d], S. Ted Oyama [a,d,*]

[a] *Research Institute for Innovation in Sustainable Chemistry, National Institute of Advanced Industrial Science and Technology, AIST Tsukuba West, 16-1 Onogawa, Tsukuba, Ibaraki 305-8569, Japan*
[b] *Zhejiang Key Laboratory for Reactive Chemistry on Solid Surfaces, Institute of Physical Chemistry, Zhejiang Normal University, Jinhua 321004, China*
[c] *Chengdu Institute of Organic Chemistry, Chinese Academy of Sciences, Chengdu 610041, China*
[d] *Environmental Catalysis and Nanomaterials Laboratory, Department of Chemical Engineering (0211), Virginia Polytechnic Institute and State University, Blacksburg, VA 24061, USA*

Available online 13 March 2007

Abstract

The oxidation of propylene to propylene oxide (PO) with hydrogen–oxygen mixtures was studied on gold supported on the mesoporous titanium silicate, Ti-TUD. The catalyst gave stable activity at low conversions of propylene (<6%) and high selectivity to PO (>95%). Kinetic data were fit to a power-rate law and gave the following expression: $r_{PO} = k(H_2)^{0.54}(O_2)^{0.24}(C_3H_6)^{0.36}$. The fractional orders in hydrogen, oxygen, and propylene indicated that these reactants interacted with the catalyst to form species that led to the final PO product. The catalyst likely operated by the commonly accepted mechanism of hydrogen peroxide production on gold sites, and epoxidation on titanium centers. Carbon dioxide was formed primarily from further oxidation of PO rather than the oxidation of propylene, while water was produced from the reaction of hydrogen and oxygen.

Keywords: Gold; Titanosilicate; Propylene oxide; Kinetics

1. Introduction

Propylene oxide (PO) is an important commodity chemical used in the production of propylene glycol and polyurethanes [1]. PO is currently produced by several indirect methods, such as the chlorohydrin process, which uses Cl_2 and H_2O, or variations of the Halcon process, which use organic hydroperoxides. These methods of production are inefficient. The chlorohydrin route produces stoichiometric amounts of salts, and the hydroperoxide routes produce co-products like *t*-butyl alcohol and styrene monomer, which have lower market demand than PO.

The direct oxidation of propylene with molecular O_2 is most desirable, but remains an elusive goal because of the high reactivity of the allylic hydrogens in propylene which lead to complete oxidation. Catalysts for direct epoxidation include $Ag/CaCO_3$ catalysts developed by ARCO [2–4], which have a selectivity as high as 60% at a conversion of 1%. Recently, Dow and BASF [5] and separately Degussa, Headwaters, and Uhde [6] have announced a new process for propylene oxide (PO) production based on the oxidation of propylene with hydrogen peroxide using TS-1 or titanosilicate catalysts. Earlier work had also reported the production of PO with H_2/O_2 mixtures using finely dispersed gold supported on titania [7]. This was followed by many other studies with H_2/O_2 mixtures using gold supported on microporous and mesoporous titanosilicates [8–10].

The Au–Ti systems studied initially mostly had excellent selectivity (>90%) at low conversion (1–3%), but all suffered from deactivation in the order of hours [8–11]. The origin of the

* Corresponding author at: Environmental Catalysis and Nanomaterials Laboratory, Department of Chemical Engineering (0211), Virginia Polytechnic Institute and State University, Blacksburg, VA 24061, USA.
Tel.: +1 540 231 5309; fax: +1 540 231 5022.
E-mail address: oyama@vt.edu (S.T. Oyama).

0920-5861/$ – see front matter © 2007 Elsevier B.V. All rights reserved.
doi:10.1016/j.cattod.2007.02.005

deactivation is likely to be strongly adsorbed PO species [12–15], not sintering of gold, and probably occurs on multiply coordinated Ti centers (Ti–O–Ti) [12,16]. This has been overcome by the use of highly dispersed gold on titania–silica [12] and TS-1 [12,17–19] supports with moderately low Ti contents. Using the latter catalyst the kinetics of the PO reaction was recently investigated [20] and the PO formation rate was found to follow a power-rate law of the form $r_{PO} = k(H_2)^{0.60}(O_2)^{0.31}(C_3H_6)^{0.18}$.

In this study the kinetics are examined on another stable catalyst system, gold supported on the mesoporous titanosilicate, Ti-TUD. The catalyst contains barium as a promoter, which improves the conversion by increasing the gold loading. The rate expression obtained is similar, $r_{PO} = k(H_2)^{0.54}(O_2)^{0.24}(C_3H_6)^{0.36}$, and this suggests that the catalyst operates by a similar mechanism.

2. Experimental

2.1. Catalyst preparation

The Ti-TUD support with a Ti content of 3 mol% was prepared by a modified sol–gel method following a procedure reported in the literature [21,22]. The resulting material has a specific surface area of 501 $m^2\ g^{-1}$ and an average pore size of 13 nm.

The Au supported Ti-TUD catalysts were prepared using a deposition–precipitation method (DP) [23]. In a typical preparation 100 ml of 2.4 mM $HAuCl_4.4H_2O$ solution was heated to 343 K under vigorous stirring. The pH of the solution was adjusted to 8.9 using a 1 M Na_2CO_3 solution. Following this, 1 g of the support was added and the suspension was stirred for 15 min. Then 0.19 mmol of $Ba(NO_3)_2$ (99.0%) dissolved in 5 ml H_2O was added and the mixture was stirred for another 45 min at the same temperature and pH. The solid was filtered and washed with 100 ml of Millipore H_2O, dried under vacuum for 12 h, and then calcined in air at 573 K for 4 h. The sample was designated Au–Ba/Ti-TUD (9), where the number in parentheses refers to the final pH during preparation. The loadings of Au and Ba in the catalyst were 0.11 and 2.4 wt%, respectively, determined by inductively coupled plasma (ICP) analysis.

2.2. Catalytic testing

The epoxidation of propylene was carried out in a quartz tubular microreactor of 6 mm diameter and 180 mm length using 0.3 g catalyst of 100–140 mesh size without dilution. Flow rates of Ar (99.9%), O_2 (99.5%), H_2 (99.5%) and C_3H_6 (99.8%) were 24.5, 3.5, 3.5 and 3.5 $cm^3\ min^{-1}$ each and were controlled by mass flow meters, with the reaction pressure set at 0.1 MPa. The space velocity was 7000 $cm^3\ h^{-1}\ g\text{-}cat^{-1}$. Before reaction the catalyst was pretreated with 13 vol.% H_2 in Ar (27 $cm^3\ min^{-1}$) and 13 vol.% O_2 in Ar (27 $cm^3\ min^{-1}$) at 523 K for 0.5 h, respectively, after which the temperature was set to 423 K and the reactants were introduced. Reaction products were analyzed online using two gas chromatographs (Shimazu GC-14) using Ar as the carrier gas. Each of them was equipped with a flame ionization detector (FID) and a thermal conductivity detector (TCD). One had a FFAP capillary column (0.32 mm × 60 m) and a Porapak Q compact column (3 mm × 2 m). The other had a Gaskuropak 54 84/100 compact column (3 mm × 2 m) and a MS-5A 60/80 compact column (3 mm × 2 m). The FFAP capillary column and Porapak Q were used to detect oxygenates (acetaldehyde, PO, acetone, propionaldehyde, acrolein, acetic acid and isopropanol) and CO_2 and H_2O, respectively. The Gaskuropak and MS-5A columns were used to detect hydrocarbons (propane, propylene, ethylene and ethane) and H_2, O_2 and CO, respectively. Carbon balances were close to 100 ± 3%. The propylene conversion, PO selectivity, H_2 conversion, and H_2 selectivity were defined as follows:

$$\text{propylene conversion} = \frac{\text{moles of (oxygenates} + CO_2/3)}{\text{moles of propylene in feed}}$$

$$\text{PO selectivity} = \frac{\text{moles of PO}}{\text{moles of (oxygenates} + CO_2/3)}$$

$$H_2\ \text{conversion} = \frac{\text{moles of } H_2 \text{ in feed} - \text{moles of } H_2 \text{ in product}}{\text{moles of } H_2 \text{ in feed}}$$

$$H_2\ \text{selectivity} = \frac{\text{moles of PO}}{\text{moles of } H_2O}$$

The kinetic study was initiated after the reaction reached steady-state, which took about 6 h. Partial pressure dependencies of the reaction rates were measured by varying the flow rate of each reactant, while keeping the total flow rate at 35 $cm^3\ min^{-1}$ by adjusting the flow rate of Ar. A factorial design methodology [24] was used to obtain rate parameters at 443 K over a moderately large range of reactant partial pressures. Three levels of partial pressures were used for H_2, O_2 and C_3H_6: low (L = 2.9 kPa), medium (M = 10.1 kPa) and high (H = 20.2 kPa). The partial pressures were varied so that in parameter space the H and L values were placed at the vertices of a cube and the M values were located on the face midpoints and the cube center point. Some of the combinations of the partial pressures were in the flammable regime, but no ignition was observed. Limited measurements were carried out at other temperatures (423 and 463 K). Each measurement was taken after stable rates were achieved, which took about 1 h. The order of experiments was varied randomly in order not to introduce bias in the results, but the highest temperature point was taken first in order to minimize possible catalyst changes. Lack of deactivation was verified by repeating an initial measurement at the end of the experiments and checking that conversion and selectivity had not been reduced. The power-rate law expressions were obtained by taking partial pressures of each reactant (kPa) and the formation rate (mmol h^{-1} kg-cat^{-1}) data and simultaneously fitting the entire dataset by linear least squares regression analysis using the POLYMATH 5.1 program [25].

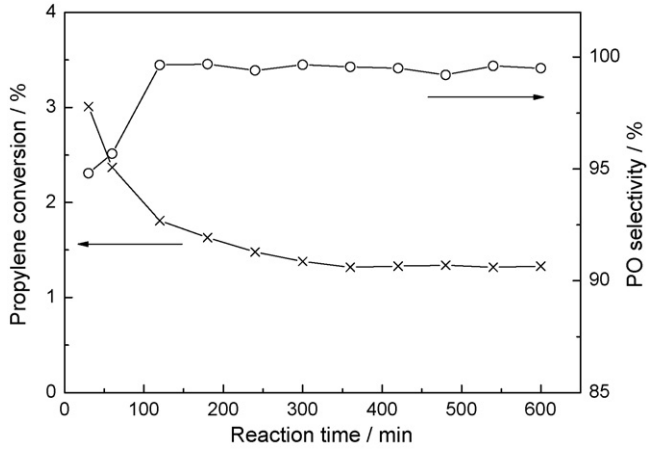

Fig. 1. Propylene conversion and PO selectivity over the Au–Ba/Ti-TUD (9) catalyst with reaction time on stream. Reaction conditions: $C_3H_6/H_2/O_2/Ar = 3.5/3.5/3.5/24.5$ cm^3 min^{-1}, S.V. = 7000 cm^3 h^{-1} g-cat^{-1}, $T = 423$ K, $P = 0.1$ MPa.

3. Results

A full report of the preparation and characterization of the Au–Ba/Ti-TUD catalyst will be presented elsewhere. Briefly, ultraviolet–visible (UV–vis) spectrum of the support shows a broad band at 230 nm, which is characteristic of tetrahedrally coordinated Ti species in the silica matrix [26–28]. High-resolution transmission electron microscopy of the catalyst shows the absence of gold particles of size larger than 2 nm (the instrumental resolution) indicating that the gold is finely dispersed. Fig. 1 shows the reactivity over the Au–Ba/Ti-TUD (9) catalyst as a function of reaction time. The initial propylene conversion was 3.0%, but decreased with reaction time to reach a steady-state value of 1.4% after 6 h. The PO selectivity, however, was extremely high (almost 100%) at steady-state.

Table 1 summarizes catalytic results over the Au–Ba/Ti-TUD (9) catalyst with various combinations of reactant partial pressures. Propylene conversion tracked ratios of $C_3H_6/H_2/O_2$ in the feedstream. It should be noted that the PO production rate is not proportional to the propylene conversion reported in the table because different inlet propylene partial pressures were used. In general, it is observed that with increasing H_2 and O_2 partial pressures the propylene reaction rate increases, while PO selectivity declines, and CO_2 selectivity rises (runs 1, 3 and 5). Table 1 also reports hydrogen efficiency, defined as the ratio of the amounts of PO and H_2O formed.

Table 2 lists the PO formation rate dependency on the entrance nominal partial pressures of H_2, O_2 and C_3H_6 as a power law expression $r_{PO} = k(H_2)^a(O_2)^b(C_3H_6)^c$, together with error analysis results for the fitting. Since PO could be involved in the CO_2 and H_2O formation, the dependencies of these on PO were also considered. The results are given below for the rates of PO formation (r_{PO}), CO_2 formation (r_{CO_2}), and H_2O formation (r_{H_2O}):

$$r_{PO} = k_{PO}(H_2)^{0.54}(O_2)^{0.24}(C_3H_6)^{0.36} \quad (1)$$

$$r_{CO_2} = k_{CO_2}(H_2)^{0.52}(O_2)^{0.27}(C_3H_6)^{0.073} \quad (2)$$

$$r_{H_2O} = k_{H_2O}(H_2)^{0.67}(O_2)^{0.16}(C_3H_6)^{0.030} \quad (3)$$

Table 2 also lists the dependencies of the rates of CO_2, and H_2O formation on other combinations of reactant and product compositions. These will be covered in Section 4.

Fig. 2 presents parity plots and residuals comparing the experimental formation rates for PO, CO_2 and H_2O with the

Table 1
Summary of catalytic results with various combinations of reactants at 443 K

Run	Partial pressure (kPa)			C_3H_6 conversion (%)	Selectivity (%)					H_2 efficiency (%)	Formation rate (mmol h^{-1} kg-cat^{-1})		
	C_3H_6	H_2	O_2		PO	PA	Ac	An	CO_2		PO	CO_2	H_2O
1	2.9	2.9	2.9	1.2	96.2	0	1.7	2.1	0	7.3	103	0	1410
2	2.9	2.9	20.2	1.8	95.0	0	0.9	4.1	0	8.6	153	0	1760
3	2.9	20.2	2.9	3.4	85.9	0.9	2.4	0	10.8	5.2	261	32.7	5010
4	2.9	10.1	10.1	3.1	85.7	0	1.9	1.0	11.4	6.7	237	31.7	3540
5	2.9	20.2	20.2	5.8	86.7	0.6	1.2	0.5	11.0	6.0	449	57.2	7480
6	10.1	2.9	10.1	0.8	94.4	0	0.5	5.1	0	11.5	236	0	2050
7	10.1	10.1	2.9	1.1	89.3	0	2.7	0	8.0	9.1	307	27.6	3370
8	10.1	10.1	10.1	1.5	91.2	0	0.4	1.5	6.9	13.0	428	32.3	3290
9	10.1	10.1	20.2	1.7	88.1	0	1.6	2.0	8.3	11.1	468	44.3	4220
10	10.1	20.2	10.1	2.3	90.6	0	1.6	0	7.8	8.8	651	56.0	7400
11	20.2	2.9	2.9	0.3	100	0	0	0	0	13.0	188	0	1440
12	20.2	2.9	20.2	0.5	92.9	0	0	7.1	0	14.1	290	0	2060
13	20.2	10.1	10.1	0.8	90.8	0	0	2.2	7.0	13.0	454	34.8	3490
14	20.2	20.2	2.9	1	90.8	0	3.1	0	6.1	10.5	567	38.2	5400
15	20.2	20.2	20.2	1.6	92.5	0	0.1	1.0	6.4	12.4	925	64.3	7460
16	10.1	10.1	10.1	1.4	88.8	0	1.0	1.6	8.6	10.2	388	37.5	3810
17[a]	10.1	10.1	10.1	2.7	84.8	0	1.3	2.6	11.3	10.0	716	95.3	7160
18[b]	10.1	10.1	10.1	0.8	100	0	0	0	0	12.3	250	0.0	2030

PO, propylene oxide; PA, propionaldehyde; Ac, acetone; An, acrolein.
[a] 463 K.
[b] 423 K.

Table 2
Dependencies of formation rates on nominal partial pressure of reactants

Formation	k[a]	Dependency				R^2	95% confidence			
		H_2 (a)	O_2 (b)	C_3H_6 (c)	PO (d)		H_2 (a)	O_2 (b)	C_3H_6 (c)	PO (d)
PO formation	30	0.54	0.24	0.36		0.985	0.06	0.06	0.06	
CO_2 formation	4.9	0.52	0.26	0.073		0.968	0.14	0.06	0.06	
	21		0.25	0.056		0.521		0.22	0.22	
	14	0.39	0.21		0.22	0.979	0.14	0.06		0.13
	68		0.15		0.43	0.815		0.15		0.29
	360	−0.057	0.043	−0.26	0.90	0.997	0.23	0.09	0.13	0.34
H_2O formation	560	0.67	0.16	0.030		0.978	0.07	0.07	0.07	
	600	0.67	0.16			0.976	0.07	0.07		
	810	0.60	0.12		0.13	0.981	0.11	0.08		0.17
	27,000		−0.053		0.89	0.752		0.23		0.33

Catalyst: Au–Ba/Ti-TUD (9), $T = 443$ K, $P = 0.1$ MPa and S.V. = 7000 $cm^3\ h^{-1}\ g\text{-}cat^{-1}$.
[a] Units will vary with the exponents to make the units of rate mmol h^{-1} kg-cat^{-1}.

rates calculated based on data fitting. The parity plot lines pass through the origin and show no systematic deviations. Fig. 3 shows the relationship between PO selectivity and propylene conversion. A general trend of decreasing selectivity with conversion is observed. Fig. 4 shows Arrhenius plots of the rate of H_2O, PO and CO_2 formation.

4. Discussion

As noted in Section 1, most catalysts employed for PO production using H_2/O_2 mixtures on gold catalysts suffer from deactivation [12,14,16,30], and reliable kinetic studies have not been possible. The only exceptions have been studies on highly dispersed titania–silica (Si/Ti = 80) [12] and Au/TS-1 microporous catalysts with highly dispersed gold and moderately low Ti contents [12,17,18,20] (Si/Ti = 36–143). In this work the catalyst employed was a Au/Ti-TUD mesoporous material also with well dispersed gold and a moderately low Ti content (Si/Ti = 33). The catalyst was promoted with barium, which had the effect of augmenting the rate by increasing the gold loading. The catalyst activity as a function of time (Fig. 1) shows an initial drop in activity but stabilization after 6 h. The attainment of stable activity permitted the kinetic measurements described in this study.

The maximum rate achieved on the Au–Ba/Ti-TUD catalyst was 935 mmol h^{-1} kg-cat^{-1}, corresponding to 53.7 $g_{PO}\ h^{-1}$ kg-cat^{-1}. This value is comparable to the rates reported in the literature for similar catalysts on mesoporous titanosilicates [9,29]. However, the values reported in these studies were initial reactivities, which dropped by more than half after 4 h. The

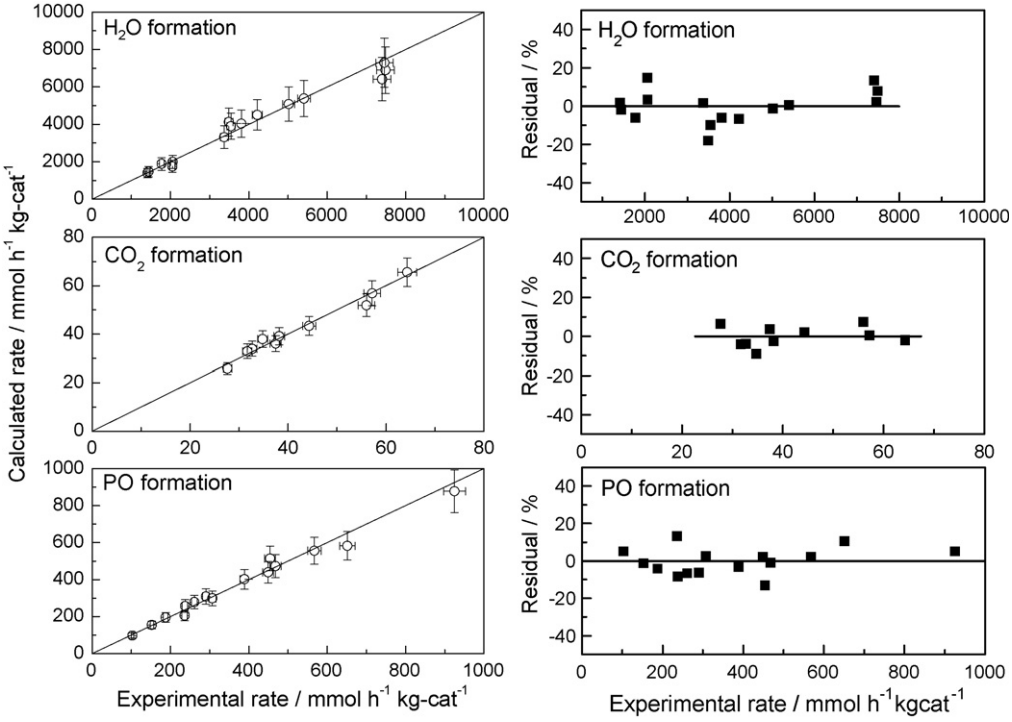

Fig. 2. Parity plots and residuals of the calculated and experimental rates.

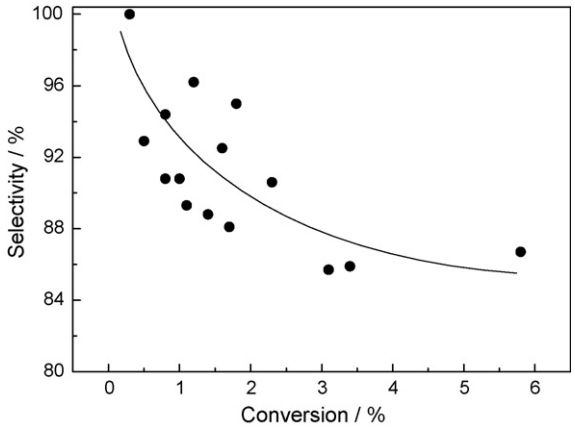

Fig. 3. Correlation between propylene oxide selectivity and conversion.

highest PO rate reported in the literature is 116 $g_{PO}\ h^{-1}\ kg\text{-}cat^{-1}$ obtained on a microporous TS-1 support [18].

The reaction rate data in this study (Table 1) was measured at low propylene conversions (1–6%). This is fairly standard in studies of the PO reaction with gold catalysts, and is actually expected because of the difficulty of the transformation. For the related ethylene oxide process the industrial conversion is ~10% with a selectivity of ~85%. It has been stated that the research targets for PO are a conversion of 10%, PO selectivity of 90%, and a hydrogen efficiency of 50% [10]. The low propylene conversions obtained were convenient because they allow the use of differential analysis to obtain rate expressions without integration. However, it should be noted that the differential analysis is an approximation, because of the higher conversions of hydrogen (5–50%) and oxygen (3–30%) than that of propylene due to the occurrence of the parallel combustion reaction. The selectivity to PO was high (>85%), while the hydrogen efficiency was low (5–13%) (Table 1). Again, such results are commonly observed for gold catalysts.

Table 1 indicates that the partial pressures of H_2 and O_2 have a very strong effect on the conversion of propylene and the rates of PO production. The highest propylene conversion of 5.8% was obtained with the highest partial pressures of H_2 and O_2 (point 5 with $C_3H_6/H_2/O_2$ = 2.9/20.2/20.2 kPa), while the lowest conversion 0.3% was obtained with the lowest partial pressures of H_2 and O_2 (point 11 with $C_3H_6/H_2/O_2$ = 20.2/2.9/2.9 kPa). This indicates that the reaction probably goes through an intermediate formed by the interaction of H_2 and O_2. The formation of a hydroperoxide species had been suggested earlier based on the finding of a D_2 kinetic isotope effect in PO formation [30], and has been detected by in situ UV–vis spectroscopy [31].

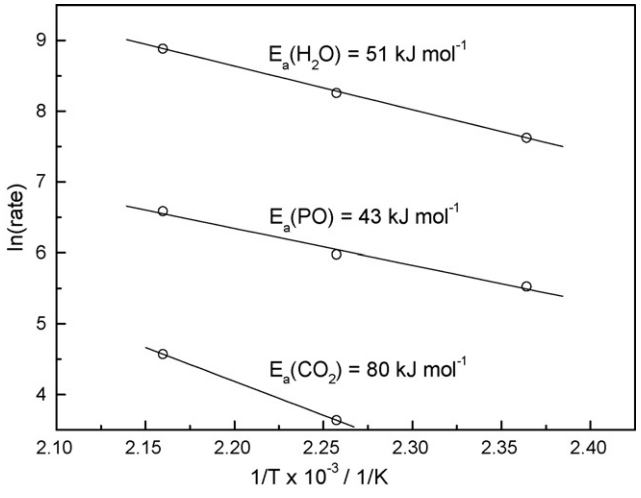

Fig. 4. Arrhenius plots of formation rates of H_2O, PO and CO_2.

Table 1 also summarizes rates of reaction as a function of the partial pressures of H_2, O_2 and C_3H_6. It shows that the rates increase as the partial pressures of each of the three reactants increases.

The rate expressions (Eqs. (1)–(3)) were calculated from regression analysis of the rate data (Table 1). The parity plots and residuals (Fig. 2) shows good agreement between measured and calculated values, indicating that the regression was successful.

For the rate of PO formation (Eq. (1)), the dependencies on H_2, O_2 and C_3H_6 were 0.54, 0.24 and 0.36, respectively (Table 2). These positive fractional orders indicate that the species are adsorbed in some manner on the catalyst surface, but not necessarily on the same sites. They also indicate that the species are involved in steps that determine the rate, but not necessarily directly. A possible reaction scheme will be discussed later.

For the CO_2 formation rate (Eq. (2)), the regression analysis shows that the formation rate dependencies on H_2, O_2 and C_3H_6 were 0.52, 0.27 and 0.073, respectively. The low value of the C_3H_6 exponent indicates that propylene is not involved in CO_2 formation. To assess the possibility that CO_2 was produced from PO, a fit of the rate data with H_2, O_2 and PO was performed. This procedure is justified because of the assumption of differential operation, which would require the PO concentration to vary linearly down the catalyst bed, with an average concentration of half the exit concentration. Taking this into consideration, the rate dependency was found to be the following:

$$r_{CO_2} = k'_{CO_2}(H_2)^{0.39}(O_2)^{0.21}(PO)^{0.22} \quad (4)$$

The order in PO was 0.22, which is larger than the order in propylene of 0.073 (Eq. (2)). This suggests that CO_2 was formed by further reaction of the produced PO rather than from propylene. The finding that the selectivity to PO decreased with increasing propylene conversion (Fig. 3) is consistent with this interpretation as higher PO levels are obtained at higher conversions, and this leads to increased CO_2. A regression was also tried for the production of CO_2 from PO with O_2 alone (Table 2), and the result was $r_{CO_2} = k''_{CO_2}(O_2)^{0.15}(PO)^{0.43}$. The main results were a decrease in the O_2 exponent from 0.21 to 0.15 and an increase in the PO exponent from 0.22 to 0.43. From these findings, it is possible to conclude that H_2 and O_2 are able to oxidize PO, but it is uncertain whether O_2 alone is involved in the oxidation, as its positive exponent appearing in the rate expression could be due to the formation of a hydroperoxide intermediate.

For H_2O formation (Eq. (3)), the formation rate dependencies on H_2, O_2 and C_3H_6 partial pressures were 0.67, 0.16 and 0.030, respectively. The very low exponent for C_3H_6 is

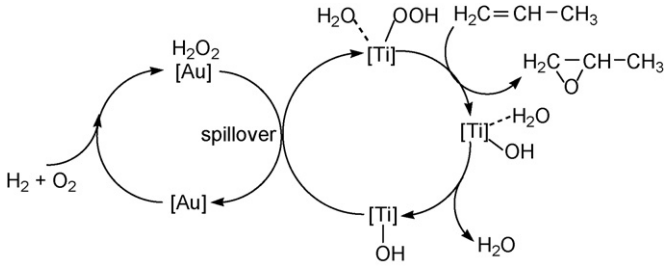

Fig. 5. Mechanism of PO formation over Au/Ti silicates (adapted from Ref. [12]).

consistent with H_2O being mainly produced by the direct reaction of H_2 and O_2. The dependency of H_2O production on the PO partial pressure was checked, and was found to yield an exponent of 0.13 (Table 2). This small value reflects the small contribution of the oxidation of PO to water formation compared to the oxidation of hydrogen.

The Arrhenius plots for the formation of H_2O, PO, and CO_2 give apparent activation energies of 51, 43, and 80 kJ mol^{-1}, respectively. The apparent activation energy for PO formation is slightly higher than the value of 35 kJ mol^{-1} reported for Au/TS-1 [20], but was close to the value of 37–41 kJ mol^{-1} for the $H_2 + O_2$ reaction [32].

A detailed interpretation of the kinetics of PO formation requires understanding of the reaction mechanism. Direct coverage of this topic is beyond the scope of this investigation, but the substantial work carried out in this area provides a basis for discussing the salient features of the mechanism.

A mechanism proposed for the PO reaction (Fig. 5) provides a beginning point for understanding the roles of gold and Ti [12]. Gold is suggested to form H_2O_2, which migrates to a Ti site with an OH group to form a hydroperoxide species responsible for epoxidation in a rate-determining step. Evidence for this scheme is that gold chemisorbs oxygen molecularly [33,34], and gold is able to produce H_2O_2 from H_2/O_2 [35–37]. The Ti is probably responsible for the PO formation as it is able to form PO with hydrogen peroxide [38]. The participation of a Ti–OH site is supported by theoretical calculations [39,40].

The kinetics of PO formation on stable Au/TS-1 catalysts has been recently reported [20] and was found to follow a power-rate law of the form $r_{PO} = k(H_2)^{0.60}(O_2)^{0.31}(C_3H_6)^{0.18}$, which is in the same range as that found here, $r_{PO} = k(H_2)^{0.54}(O_2)^{0.24}(C_3H_6)^{0.36}$. Both rate expressions feature fractional orders in reactants with the H_2 exponent about twice as large as the O_2 exponent. The propylene dependence is slightly larger for the Au/Ti-TUD catalyst. The hydrogen and oxygen dependencies are similar to those recently reported for the $H_2 + O_2$ reaction over Au/TS-1 with respective orders of 0.7–0.8 and 0.1–0.2 [32]. The latter reaction is believed to form a hydroperoxide intermediate, which is a species likely involved in the epoxidation reaction.

In the previous study on the Au/TS-1 catalyst the observed power-rate law expression was explained as originating from Langmuir–Hinshelwood type expressions for the formation of hydrogen peroxide on one site and the adsorption of propylene on another site with a single rate-determining step for PO formation involving both sites [20]. It was further assumed that both sites are adjacent.

It is possible to derive a power-rate law expression using a different set of elementary steps, and one such mechanism will be presented here. Details of the derivation of the power-rate law are presented in Appendix. The basic assumptions are:

(1) Adsorption of H_2 and O_2 occurs on different sites on gold and is equilibrated.
(2) The rate-determining step for hydrogen peroxide synthesis on gold involves the reaction of an adsorbed hydroperoxide species and molecular hydrogen.
(3) The hydrogen peroxide transfers to a Ti site with an OH group.
(4) The hydrogen peroxide on Ti forms a hydroperoxide group and an adsorbed H_2O molecule.
(5) Propylene adsorbs in an equilibrated step on the Ti site.
(6) The rate-determining step for PO production on the Ti site involves the reaction of the adsorbed propylene and hydroperoxide group.
(7) The decomposition of hydrogen peroxide to water occurs by a parallel first-order pathway:

$$O_2 + * \rightleftharpoons O_2* \quad \text{(H-1)}$$

$$H_2 + {}^{\bullet} \rightleftharpoons 2H^{\bullet} \quad \text{(H-2)}$$

$$O_2* + H^{\bullet} \rightleftharpoons HOO* + {}^{\bullet} \quad \text{(H-3)}$$

$$HOO* + H_2 + {}^{\bullet} \rightarrow H_2O_2 + * + H^{\bullet} \quad \text{(H-4)}$$

This first part of the mechanism (Eqs. (H-1)–(H-4)) involves the formation of hydrogen peroxide on two types of gold sites as was suggested in a detailed study of the kinetics and mechanism of the H_2 oxidation reaction [32]. The last part of the mechanism (Eqs. (P-1)–(P-5)) involves the formation of PO on Ti sites capable of adsorbing propylene and hydrogen peroxide (which transforms to a hydroperoxide):

$$H_2O_2 + Ti(OH) \rightleftharpoons Ti(OH)(HOOH) \quad \text{(P-1)}$$

$$Ti(OH)(HOOH) \rightleftharpoons Ti(OH_2)(OOH) \quad \text{(P-2)}$$

$$Ti(OH_2)(OOH) + C_3H_6 \rightleftharpoons Ti(OH_2)(OOH)(C_3H_6) \quad \text{(P-3)}$$

$$Ti(OH_2)(OOH)(C_3H_6) \rightarrow Ti(OH_2)(OH)(C_3H_6O) \quad \text{(P-4)}$$

$$Ti(OH_2)(OH)(C_3H_6O) \rightleftharpoons Ti(OH) + H_2O + C_3H_6O \quad \text{(P-5)}$$

Assuming that also hydrogen peroxide can decompose to water by a parallel first-order pathway, it is possible to derive a power-rate law expression of the form $r_{PO} = k(H_2)^k(O_2)^l(C_3H_6)^m$. A key aspect of this mechanism is that there are two irreversible steps that jointly determine the rate. One is involved in the production of hydrogen peroxide on a gold site, and the other is involved with the epoxidation of propylene with a hydroperoxide species on a Ti site. The presence of a single rate-determining step on a single site was considered, and found to be inconsistent with the kinetics as previously reported [20], as this would result in an order of H_2 equal to O_2 or one-half of O_2.

As mentioned earlier for the rate of PO formation (Eq. (1)), the dependencies on H_2, O_2 and C_3H_6 were 0.54, 0.24 and

0.36, respectively (Table 2). The exact meaning of the exponents cannot be determined without evaluating all the constants in the rate expression (Appendix), and this cannot be done in the present case for lack of sufficient data. However, since the rate expression contains terms that are approximately of the Langmuir–Hinshelwood type with general form $K[A]/(1 + K[A])$ the size of the exponents should roughly be inversely related to the amount adsorbed. Thus, the amount adsorbed should decrease in the order $O_2 > C_3H_6 > H_2$.

Although the kinetics obtained in the present study on Au/Ti-TUD are close to those obtained in the previous work on Au/TS-1 [20], the findings here provide only limited information about the details of the mechanism. Although it is likely that the mechanism is similar, involving separate gold sites for the formation of hydrogen peroxide, and titania sites for the epoxidation reaction (Fig. 5), it is uncertain whether the sites need to be adjacent, or whether a single rate-determining step exists. The details for this mechanism require more in-depth studies of adsorption and spectroscopic probing of the reaction intermediates.

5. Conclusions

A gold catalyst supported on the mesoporous titanosilicate Ti-TUD was found to be a stable catalyst for the formation of propylene oxide (PO) with hydrogen and oxygen as a mixed oxidant. Kinetic data were well described by a power-rate law of the form $r_{PO} = k(H_2)^{0.54}(O_2)^{0.24}(C_3H_6)^{0.36}$. Apparent activation energies for the formation of H_2O, PO and CO_2 were 51, 43, and 80 kJ mol^{-1}, respectively. Carbon dioxide was found to be formed from the further oxidation of PO rather than the oxidation of propylene. Water was found to be formed principally from the reaction between hydrogen and oxygen. The kinetic results are consistent with a mechanism involving the production of hydrogen peroxide on gold and the epoxidation of propylene on titanium centers.

Acknowledgements

The authors are grateful for financial support from the Ministry of Economy, Trade and Industry (METI, Minimum energy chemistry project) and the National Science Foundation. J.J.B.-S. acknowledges financial support from the Japan Society for the Promotion of Science (JSPS) through the Postdoctoral Fellowships for Foreign Researchers Program (No. P05627).

Appendix A

For the hydrogen peroxide sequence equilibrium relations (Eqs. (H-1)–(H-4)) yield:

$$(O_2*) = K_1(O_2)(*)$$

$$(H) = K_2^{1/2}(H_2)^{1/2}(^\bullet)$$

$$(^\bullet)(HOO*) = K_3(^*O_2)(H^\bullet)$$

$$(HOO*) = K_3(^*O_2)(H^\bullet)(^\bullet)^{-1}$$

$$(HOO*) = K_1K_3(O_2)(*)(H^\bullet)(^\bullet)^{-1}$$

$$(HOO*) = K_1K_2^{1/2}K_3(O_2)(*)(H_2)^{1/2}$$

Site balance for oxygen sites yields:

$$(L_O) = (*) + (O_2*) + (HOO*)$$

$$(L_O) = (*) + K_1(O_2)(*) + K_1K_2^{1/2}K_3(O_2)(H_2)^{1/2}(*)$$

$$(L_O) = (*)\lfloor 1 + K_1(O_2) + K_1K_2^{1/2}K_3(O_2)(H_2)^{1/2}\rfloor$$

Site balance for hydrogen sites yields:

$$(L_H) = (^\bullet) + (H^\bullet)$$

$$(L_H) = (^\bullet) + K_2^{1/2}(H_2)^{1/2}(^\bullet)$$

$$(L_H) = (^\bullet)\lfloor 1 + K_2^{1/2}(H_2)^{1/2}\rfloor$$

The reaction rate is given by:

$$r_{HOOH} = k_4(HOO*)(H_2)(^\bullet)$$

$$r_{HOOH} = k_4K_1K_2^{1/2}K_3(O_2)(H_2)^{3/2}(*)(^\bullet)$$

$$r_{HOOH} = \frac{k_4K_1K_2^{1/2}K_3(O_2)(H_2)^{3/2}(L_O)(L_H)}{[1 + K_1(O_2) + K_1K_2^{1/2}K_3(O_2)(H_2)^{1/2}] \times [1 + K_2^{1/2}(H_2)^{1/2}]}$$

$$r_{HOOH} = \frac{\alpha(O_2)(H_2)^{3/2}}{[1 + \beta(O_2) + \gamma(O_2)(H_2)^{1/2}][1 + \delta(H_2)^{1/2}]}$$

For the PO sequence (Eqs. (P-1)–(P-5)), the nomenclature can be simplified as follows:

$$I + S \rightleftharpoons S_1 \quad \text{(A-1)}$$

$$S_1 \rightleftharpoons S_2 \quad \text{(A-2)}$$

$$S_2 + C \rightleftharpoons S_3 \quad \text{(A-3)}$$

$$S_3 \rightleftharpoons S_4 \quad \text{(A-4)}$$

$$S_4 \rightleftharpoons S + W + P \quad \text{(A-5)}$$

where I = H_2O_2, C = C_3H_6, W = H_2O, P = C_3H_6O. S is the bare Ti site and S_{1-4} are the surface intermediates.

The RDS gives:

$$r_P = k'_4(S_3)$$

Equilibrium balances yield:

$$(S_1) = K'_1(I)(S)$$

$$(S_2) = K'_2(S_1) = K'_1K'_2(I)(S)$$

$$(S_3) = K'_3(C)(S_2) = K'_2K'_3(C)(S_1) = K'_1K'_2K'_3(C)(I)(S)$$

Site balance yields:

$$(L) = (S) + (S_1) + (S_2) + (S_3)$$

$$(L) = (S) + K'_1(I)(S) + K'_1K'_2(I)(S) + K'_1K'_2K'_3(C)(I)(S)$$

$$(L) = (S)[1 + K'_1(I) + K'_1K'_2(I) + K'_1K'_2K'_3(C)(I)]$$

$$r_{PO} = k'_4K'_1K'_2K'_3(C)(I)(S)$$

$$r_{PO} = \frac{k'_4k'_1k'_2k'_3(C)(I)(L)}{[1 + k'_1(I) + k'_1k'_2(I) + k'_1k'_2k'_3(C)(I)]}$$

$$r_{PO} = \frac{\kappa(C)(I)}{[1 + \lambda(I) + \mu(C)(I)]}$$

Combining the equations and accounting for a first-order decomposition:

$$r_{HOOH} = \frac{\alpha(O_2)(H_2)^{3/2}}{[1 + \beta(O_2) + \gamma(O_2)(H_2)^{1/2}][1 + \delta(H_2)^{1/2}]} \quad \text{(A-6)}$$

$$r_{PO} = \frac{\kappa(C_3H_6)(HOOH)}{[1 + \lambda(HOOH) + \mu(C_3H_6)(HOOH)]} \quad \text{(A-7)}$$

$$r_{HOOH} = r_{PO} + r_{decomp} = r_{PO} + k_D(HOOH) \quad \text{(A-8)}$$

$$\frac{\alpha(O_2)(H_2)^{3/2}}{[1 + \beta(O_2) + \gamma(O_2)(H_2)^{1/2}][1 + \delta(H_2)^{1/2}]} = \frac{\kappa(C_3H_6)(HOOH)}{[1 + \lambda(HOOH) + \mu(C_3H_6)(HOOH)]} + k_D(HOOH)$$

$$\text{Let } M = \frac{\alpha(O_2)(H_2)^{3/2}}{[1 + \beta(O_2) + \gamma(O_2)(H_2)^{1/2}][1 + \delta(H_2)^{1/2}]}$$

$$M[1 + \lambda(HOOH) + \mu(C_3H_6)(HOOH)] = \kappa(C_3H_6)(HOOH) + k_D(HOOH)[1 + \lambda(HOOH) + \mu(C_3H_6)(HOOH)]$$

$$M + M\lambda(HOOH) + M\mu(C_3H_6)(HOOH) = \kappa(C_3H_6)(HOOH) + k_D(HOOH) + k_D\lambda(HOOH)^2 + k_D\mu(C_3H_6)(HOOH)^2$$

This can be expressed as:

$$a(HOOH)^2 + b(HOOH) + c = 0$$

where $a = k_D\lambda + k_D\mu(C_3H_6)$, $b = \kappa(C_3H_6) + k_D - M\lambda - M\mu(C_3H_6)$ and $c = M$.

The solution is:

$$(HOOH) = f_1[(H_2), (O_2), (C_3H_6)]$$

where f_1 is an algebraic equation.

Substituting in the expression for the rate of PO formation:

$$r_P = \frac{\kappa(C_3H_6)\, f_1}{[1 + \lambda\, f_1 + \mu(C_3H_6)\, f_1]}$$

which is another algebraic equation which can approximated by a power-rate law form:

$$r_P = k(H_2)^k(O_2)^l(C_3H_6)^m$$

Note that Eq. (A-7) can be simplified if it is assumed that the right terms in the denominator $\lambda(HOOH) + \mu(C_3H_6)(HOOH)$ are all much smaller than 1 (possibly if H_2O_2 concentration is quite small, which is reasonable):

$$r_{PO} = \kappa(C_3H_6)(HOOH) \quad \text{(A-9)}$$

Solving for HOOH using Eq. (A-8):

$$(HOOH) = \frac{r_{HOOH}}{[k_D + \kappa(C_3H_6)]} \quad \text{(A-10)}$$

Substituting Eqs. (A-6) and (A-10) in Eq. (A-9):

$$r_{PO} = \frac{(C_3H_6)}{[k_D/\kappa + (C_3H_6)]} \times \frac{\alpha(O_2)(H_2)(H_2)^{1/2}}{[1 + \beta(O_2) + \gamma(O_2)(H_2)^{1/2}][1 + \delta(H_2)^{1/2}]} \quad \text{(A-11)}$$

Eq. (A-11) is an expression similar (right term only) to the rate of formation of H_2O obtained earlier [32], and their arguments for the further simplification of this expression can also be used: assuming that the $\delta(H_2)^{1/2}$ term is larger than 1, it will cancel the $(H_2)^{1/2}$ term in the numerator. Then orders for O_2 and C_3H_6 will be between 0 and 1 and for H_2 between 0.5 and 1.

References

[1] D.L. Trent, Propylene Oxide in Kirk Othmer Encyclopedia of Chemical Technology, on-line ed., John Wiley and Sons, New York, 2001.
[2] S.T. Oyama, K. Murata, M. Haruta, Shokubai 46 (2004) 13.
[3] J. Lu, J.J. Bravo-Suárez, A. Takahashi, M. Haruta, S.T. Oyama, J. Catal. 232 (2005) 85.
[4] J. Lu, J.J. Bravo-Suárez, M. Haruta, S.T. Oyama, Appl. Catal. A 302 (2006) 283.
[5] A. Tullo, BASF, Dow plan more propylene oxide units, Latest News Chem. Eng. News, October 31, 83 (44) (2005) 7.
[6] News from Achema 2006, New method for manufacturing propylene oxide eliminates undesirable side products, Chem. Eng. Prog. (2006) 13.
[7] T. Hayashi, K. Tanaka, M. Haruta, J. Catal. 178 (1998) 566.
[8] B.S. Uphade, S. Tsubota, T. Hayashi, M. Haruta, Chem. Lett. (1998) 1277.
[9] A.K. Sinha, S. Seelan, S. Tsubota, M. Haruta, Angew. Chem. Int. Ed. 43 (2004) 1546.
[10] A.K. Sinha, S. Seelan, M. Okumura, T. Akita, S. Tsubota, M. Haruta, J. Phys. Chem. B 109 (2005) 3956.
[11] B.S. Uphade, Y. Yamada, T. Akita, T. Nakamura, M. Haruta, Appl. Catal. A 215 (2001) 137.
[12] T.A. Nijhuis, B.J. Huizinga, M. Makkee, J.A. Moulijn, Ind. Eng. Chem. Res. 38 (1999) 884.
[13] B.S. Uphade, M. Okumura, S. Tsubota, M. Haruta, Appl. Catal. A 190 (2000) 43.
[14] B.S. Uphade, T. Akita, T. Nakamura, M. Haruta, J. Catal. 209 (2002) 331.
[15] A. Swijnenburg, M. Makkee, J.A. Moulijn, Appl. Catal. A 270 (2004) 49.
[16] G. Mul, A. Zwijnenburg, B. van der Linden, M. Makkee, J.A. Moulijn, J. Catal. 201 (2001) 128.
[17] N. Yap, R.P. Andres, W.N. Delgass, J. Catal. 226 (2004) 156.
[18] B. Taylor, J. Lauterbach, W.N. Delgass, Appl. Catal. A 291 (2005) 188.
[19] E.E. Stangland, B. Taylor, R.P. Andres, W.N. Delgass, J. Phys. Chem. B 109 (2005) 2321.
[20] B. Taylor, J. Lauterbach, G.E. Blau, W.N. Delgass, J. Catal. 242 (2006) 142.
[21] J.C. Jansen, Z. Shan, L. Marchese, W. Zhou, N.V.D. Puil, T. Maschmeyer, Chem. Commun. 8 (2001) 713.
[22] Z. Shan, E. Gianotti, J.C. Jansen, J.A. Peters, L. Marchese, T. Maschmeyer, Chem. Eur. J. 7 (2001) 1437.

[23] S. Tsubota, D.A.H. Cunningham, Y. Bando, M. Haruta, Stud. Surf. Sci. Catal. 91 (1995) 227.
[24] L. Ott, An Introduction to Statistical Methods and Data Analysis Analysis, 3rd ed., PWS-Kent, Boston, 1992.
[25] M. Shacham, M.B. Cutlip, M. Elly, Polymath, Copyright 2006.
[26] T. Blasco, A. Corma, M.T. Navarro, J.P. Pariente, J. Catal. 156 (1995) 65.
[27] M.D. Alba, Z. Luan, J. Klinowski, J. Phys. Chem. 100 (1996) 2178.
[28] S. Gontier, A. Tuel, J. Catal. 157 (1995) 24.
[29] B. Chowdhury, J.J. Bravo-Suárez, M. Daté, S. Tsubota, M. Haruta, Angew. Chem. Int. Ed. 45 (2006) 412.
[30] E.E. Stangland, K.B. Stavens, R.P. Andres, W.N. Delgasss, J. Catal. 191 (2000) 332.
[31] B. Chowdhury, J.J. Bravo-Suárez, N. Mimura, J.Q. Lu, K.K. Bando, S. Tsubota, M. Haruta, J. Phys. Chem. B 110 (2006) 22995.
[32] D.G. Barton, S.G. Podkolzin, J. Phys. Chem. B 109 (2005) 2262.
[33] S. Naito, M. Tanimoto, J. Chem. Soc. Chem. Commun. (1988) 832.
[34] M. Okumura, J.M. Coronado, J. Soria, M. Haruta, J.C. Conesa, J. Catal. 203 (2001) 168.
[35] P.P. Oliveira, E.M. Patrito, H. Sellers, Surf. Sci. 313 (1994) 25.
[36] M. Okumura, Y. Kitagawa, K. Yamaguchi, T. Akita, S. Tsubota, M. Haruta, Chem. Lett. 32 (2003) 822.
[37] J.K. Edwards, B.E. Solsona, P. Landon, A.F. Carley, A. Herzing, C.J. Kiely, G.J. Hutchings, J. Catal. 236 (2005) 69.
[38] M.G. Clerici, G. Bellussi, U. Romano, J. Catal. 129 (1991) 159.
[39] D.H. Wells Jr., W.N. Delgass, K.T. Thomson, J. Am. Chem. Soc. 126 (2004) 2956.
[40] D.H. Wells Jr., A.M. Joshi, W.N. Delgass, K.T. Thomson, J. Phys. Chem. B 110 (2006) 14627.